Received: 10 June 2026 | Revised: 14 September 2026 | Accepted: 9 October 2026 | Published online: 30 October 2026

RESEARCH ARTICLE

Smart Wearable Technology
2026, Vol. 00(00) 1–14
DOI: 10.47852/bonviewSWT620210799

BON VIEW PUBLISHING

# Proof-of-Concept End-to-End EEG-BCI Pipeline for Grasp-and-Release Decoding and Low-Cost Tendon-Driven Actuation

**Krishnakumar Sankar[1,*], Kanimozhi Gowtheman[1], Keerthivasan Sundararajan[1] and Naresh Moorthi[1]**

[1] *Department of Biomedical Engineering, Rajalakshmi Engineering College, India*

**Abstract:** Stroke is a leading cause of long-term motor disability, inspiring research in the design of assistive and rehabilitation technologies that work in situations with limited residual muscle activity. Brain–computer interfaces (BCIs) offer a promising non-muscular pathway to translate brain activity into BCI commands. This paper presents the proof-of-concept end-to-end pipeline for the use of binary grasp-and-release Electroencephalography-Brain Computer Interface (EEG-BCI) decoding in conjunction with low-cost tendon-driven robotic hand actuation. The classification part of our pipeline has been trained on the publicly available WAY EEG Grasp-and-Lift dataset. It includes EEG recordings of performed grasp-and-lift movements of healthy participants, instead of motor-imagery movements. Eight EEG channels have been filtered, common average referenced, and normalized and then classified in a subject-independent manner using the EEGNet network. The proposed EEGNet achieved a trial-level accuracy of 74.74%, outperforming the baseline (60.38%) FBCSP + SVM classifier. In terms of hardware, the acknowledgment success rate was 98.18%, with 54 out of 55 transmitted commands recieving an ACK response. The executed-movement EEG data have been used only as a demonstration of engineering proof-of-concept for our decoding and robotic control pipeline. Motor-imagery EEG decoding, patients' evaluation, and clinical outcomes have not been considered in this study.

**Keywords:** brain–computer interface, EEG decoding, robotic hand rehabilitation, tendon-driven actuation, grasp-and-lift EEG

## 1. Introduction

Stroke remains a leading cause of death and long-term disability. The Global Burden of Disease 2021 estimates indicate approximately 93.8 million prevalent stroke cases worldwide and 160.5 million disability-adjusted life years attributable to stroke [1–3]. Advances in acute care have raised early survival to about 80%, so a large and growing population of survivors lives with residual motor impairment that reduces independence and quality of life. Upper-limb paresis is a principal target of rehabilitation, yet restoration of usable motor control remains difficult, particularly in the chronic phase [4, 5].

A clinically important subset of survivors is poorly served by Electromyography (EMG)-driven systems. When the Fugl-Meyer Assessment score falls below 20, residual voluntary muscle activity is often insufficient for reliable myoelectric control. Roughly 30–40% of chronic stroke patients fall into this severe category and are therefore ineligible for EMG-based rehabilitation. Brain–computer interfaces (BCIs) address this gap by bypassing the damaged neuromuscular pathway and translating cortical activity into device commands [6–9].

The relevance of EEG-based BCIs is due to their usefulness for post-stroke applications because they offer a non-muscular pathway to control assistive devices [10–16]. Although there are numerous papers devoted to BCI for Motor Imagery (MI) decoding, this work deals exclusively with executed movements in the form of the WAY EEG Grasp-and-Lift dataset [17]. Execution of movements produces greater sensorimotor responses compared to imagination and thus provides sufficient basis for preliminary validation of a BCI. The executed-movement EEG data are applied strictly for validation of EEG decoding and actuation algorithms; the MI paradigm and stroke patients are not involved. It was decided to use EEGNet because of its small architecture that implements temporal and depthwise separable convolution in order to extract the features of EEG signals [18]. The primary contributions of this research contain four main elements, which include (1) a minimal-channel system for improved usability and efficiency [19, 20], (2) EEGNet validation for subject-independent classification, (3) low-cost hardware integration, and (4) an end-to-end engineering proof-of-concept integrating EEG decoding with low-cost robotic actuation.

The proposed solution combines preprocessing, subject-independent classification with the use of EEGNet, decision filtering, and cost-effective robotic command transmission. It was tested only on the EEG data collected during performed movements of healthy participants as anengineering proof-of-concept motor imagery, stroke patients, and clinical assessment remain areas of future research.

***Corresponding author:** Krishnakumar Sankar, Department of Biomedical Engineering, Rajalakshmi Engineering College, India. Email: krishnakumar.s@rajalakshmi.edu.in and krishnakumarsankar30@gmail.com

© The Author(s) 2026. Published by BON VIEW PUBLISHING. This is an open access article under the CC BY License (https://creativecommons.org/licenses/by/4.0/).

## 2. Literature Review

Several EEG-based BCI systems have been explored for motor rehabilitation and control of assistive devices. Traditional solutions mainly focused on signal processing methods, including common spatial pattern (CSP) + support vector machine (SVM) and linear discriminant analysis (LDA), with studies reporting moderate classification performance in finger- and motor-imagery decoding tasks [21–23]. Deep learning approaches have subsequently been used to learn spatiotemporal EEG representations directly from the signal [24, 25]. Subject-independent approaches such as MIN2Net have specifically addressed inter-subject variability in motor-imagery EEG classification [26]. More recent architectures such as AMEEGNet incorporate attention and multiscale feature extraction [27], while generative deep learning approaches have also been explored for high-fidelity EEG generation [28]. Numerous works therefore demonstrate the continuing transition from conventional feature-engineered methods toward end-to-end and attention-based EEG decoding [24, 26, 27]. At the same time, augmented-reality-based BCI provides high accuracy in pattern recognition [29]. Brain-signal decoding has also been demonstrated for hand posture classification using cortical recordings [30]. Various EEG-controlled exoskeletons, orthoses, and robotic prostheses have been investigated for translating brain signals into assisted hand movements [31–36]. Among clinical studies and reviews, BCI-assisted rehabilitation has been evaluated in stroke populations and summarized across clinical trials, systematic reviews, and meta-analyzes [37–46]. Recent methodological developments have also addressed subject-independent motor-imagery EEG decoding using end-to-end deep learning approaches such as MIN2Net [47]. BCI-controlled hand-robot training has further been evaluated for post-stroke upper-limb motor recovery [48]. Complementary prosthetic-hand research has characterized natural hand movements and grasp-force requirements and evaluated the performance of commercially available and 3D-printable prosthetic hands [49, 50].

EEG decoding for the study of movement decoding could be divided into two major categories based on the behavioral paradigm used to stimulate neural responses. Motor-imagery studies investigate brain activity elicited by imagined movements without the actual execution of the movements. Motor-imagery decoding studies play an essential role in BCI applications, especially in patients unable to execute voluntary movements. However, executed-movement studies measure EEG signals during the actual physical execution of the movements, thus eliciting stronger sensorimotor responses, beneficial for initial algorithm development and engineering validations. Stroke rehabilitation studies form another category of executed-movement studies. However, the population included in stroke rehabilitation studies differs considerably from the population included in the present study. Therefore, executed-movement EEG studies of healthy subjects and motor-imagery EEG studies play the roles of initial algorithm validations before implementing clinical applications. The WAY EEG Grasp-and-Lift dataset utilized in the present study consists of EEG recordings from healthy subjects during the execution of grasp-and-lift movements. Therefore, all experiments performed here use executed-movement EEG.

Recent advancements in the field of motor-based BCIs using EEGs have involved improvements in subject-independent decoding, reducing the number of EEG channels, and integration with assistive and rehabilitation technologies. Wang et al. [19] discussed recent approaches to motor BCI involving upper-limb movements, highlighting the increasing use of EEG-based systems in restoring and controlling motor movements [19]. Subject-independent deep learning has been explored to address inter-subject variability, as demonstrated by MIN2Net [26]. Recent developments in EEGNet-style architectures include multi-branch, attention, and multiscale mechanisms, as demonstrated by AMEEGNet [27]. The trend is therefore clearly evident in moving from compact convolutional EEG models toward architectures designed to address inter-subject variability and richer feature representations.

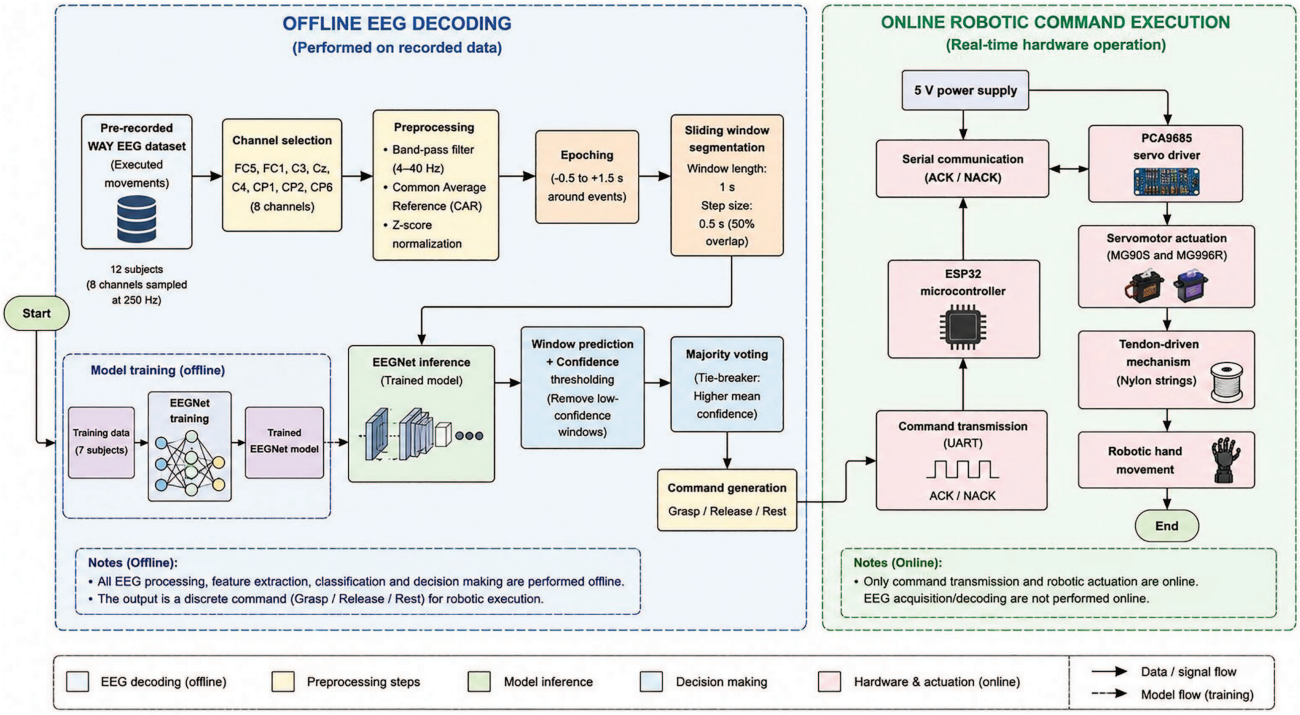
Parallel to the trend of advancements in EEG decoding techniques, researchers are integrating them with wearable and robotic rehabilitation. Fu et al. [43] demonstrated a portable BCI intervention for recovery of motor hand functions after stroke [43]. Low-cost EEG-based control of robotic hand prostheses and exoskeletons has also been demonstrated [31, 33, 36, 41, 42]. More recently, Zhang et al. [29] developed a robotic-hand prosthesis controlled using an EEG-based Augmented Reality - Steady-State Visual Evoked Potential (SSVEP) paradigm, center-Extended Canonical Correlation Analysis (ECCA-SVM) classification, and machine-vision assistance, while Ding et al. [35] demonstrated real-time EEG-based robotic hand control at the level of individual fingers [29, 35]. These studies illustrate the progression from proof-of-concept EEG-controlled devices toward more sophisticated robotic and assistive interfaces.

Nevertheless, despite these advancements, direct comparison between recently developed BCI systems becomes challenging due to different EEG paradigms used, differences in datasets, subject-independent evaluation, classification goals, and different hardware setups. Successful systems tend to use the motor-imagery paradigm, SSVEP, subject-dependent calibration, or more advanced neural architecture designs, while robotic research tends to focus on online control of robots without independent evaluation of the EEG decoding process. The current research can be regarded as an engineering proof-of-concept involving a relatively compact eight-channel EEG setup, subject-independent evaluation on the WAY Grasp-and-Lift dataset, binary classification of Grasp/Release commands using EEGNet, and implementation of a low-cost tendon-driven robotic hand. In contrast to works demonstrating continuous online EEG decoding, the current research utilizes pre-recorded EEG for classifier training and evaluation and then command transmission and robotic execution. This feature allows for separating the contribution into three distinct parts and evaluating it in terms of EEG classification, command transmission, and robotic actuation separately without claiming to have a complete continuous real-time EEG-BCI system.

## 3. Research Methodology

The proposed system integrates offline EEG signal processing with a custom-built robotic hand for Grasp/Release command generation and online robotic actuation. The overall workflow involves EEG signal preprocessing, machine learning (ML)-based classification, decision filtering, command transmission, and robotic execution. Figure 1 shows a representation of the system architecture. The proposed system combines EEG signal processing and a tendon-driven robotic hand as the proof-of-concept for grasp-and-release command generation. All EEG classification experiments were performed using EEG recordings from the WAY EEG Grasp-and-Lift dataset. There were no motor-imagery recording and stroke patient recording used in the present study. In terms of the entire procedure, it includes the steps of EEG preprocessing, window-based EEGNet classification, decision-making, command transmission, and robotic actuation. The classification was evaluated offline based on subject-independent data, whereas

**Figure 1**
**System architecture workflow for tendon-driven robotic hand actuation through BCI**




the robotic command and actuation pathway represented the hardware part of the prototype. It includes EEG signal processing, ML-based classification, hardware implementation, command creation, and robotic execution.

## 3.1. EEG dataset and signal preprocessing

### *3.1.1. Dataset description*

The EEG data employed in this research come from the freely accessible WAY EEG Grasp-and-Lift dataset that consists of multichannel EEG signals acquired at 500 Hz from 12 healthy subjects doing grasp-and-lift tasks [17]. The dataset consists of 96 EEG files and includes event markers that correspond to the various stages of the grasp-and-lift task. In the current experiment, eight EEG channels (FC5, FC1, C3, Cz, C4, CP1, CP2, and CP6) were chosen because they provide coverage of sensorimotor areas associated with the EEG signals for hand movements [20].

It should be noted that the WAY EEG Grasp-and-Lift dataset used in the current experiment includes EEG signals recorded while the subject is physically executing the movements rather than when the subject is making mental imagery of the movements. Thus, all classification experiments reported in this paper pertain to the executed-movement EEG decoding. The dataset does not contain motor-imagery recordings or recordings of stroke patients. Executed movement was chosen to assess the feasibility of the proposed pipeline for EEG preprocessing, classification, decision-generation, and robot actuation from the engineering perspective. Despite that executed movement provides relatively strong EEG responses from sensorimotor cortex, the performance obtained in this way cannot be taken as performance in motor-imagery decoding. Motor-imagery EEG validation in the clinical population is thus left for future work. An eight-channel montage was selected to see if the proposed decoding pipeline would work with a relatively compact EEG setup. However, a reduced montage may result in reduced spatial resolution compared to a high-density montage. This issue can be explored further via ablation studies.

### *3.1.2. Label definition and event-based mapping*

The WAY EEG Grasp-and-Lift database is annotated at the finest granularity level according to the phases of the grasping process, such as handStart, objectContact, loadPhase, liftOff, replace, and release. In the case of developing real-time applications for prosthetics, however, the functional description of motor intent is more appropriate than classifying actions at different phases of the grasping process. In this regard, the multiclass labels have been translated into a binary labeling scheme consistent with the operational requirements of the system. In this experiment, epochs were extracted based on the occurrence of handStart events for grasping, while for release actions, the epoch was based on the replace event. Although we only utilized the single event onsets, the selected epoch window (-0.5 s to + 1.5 s) covers the entire action sequence of grasping and lifting objects. As such, an epoch contains subsequent phases such as objectContact, loadPhase, and liftOff, providing an efficient representation of continuous movements without combining several events to obtain a labeled epoch. This binary mapping (Grasp vs. Release) is functionally relevant for prosthetic control, although it simplifies the rich multi-phase annotation of the original dataset.

Inclusion of forearm rotation in the actuation scheme does not qualify as another separate class but rather is considered a continuation of the process of grasping itself. Biomechanically, human grasping is a coordination of the wrist and forearm movements, especially at the moment of lift-off. Rotation is not specifically modeled like other events; it was included within each event's time window. This is due to the nature of motor-related EEG activity, being continuous rather than characterized by phase transitions. There is evidence from previous studies showing similar characteristics of Event-Related Desynchronization/

Event-Related Synchronization (ERD/ERS) in both $\mu$ and $\beta$ bands in relation to grasp phases [50].

The WAY-EEG-GAL dataset is annotated at fine-temporal granularity across grasp-and-lift phases, including HandStart, FirstDigitTouch (object contact), BothStartLoadPhase, LiftOff, Replace, and BothReleased [17]. The robotic prototype used here, however, accepts only two functional commands—Grasp and Release. Multi-phase labels were therefore mapped to a binary scheme aligned with this actuation interface rather than retained as a six-class phase decoder.

Event onsets served only as temporal anchors for epoching, not as instantaneous classification targets. Grasp epochs were locked to HandStart, which marks the onset of reach toward the object. Release epochs were locked to Replace, which marks the start of object return and hand withdrawal. Each epoch spanned −0.5 s to + 1.5 s relative to the selected onset. Consequently, a HandStart-locked Grasp window still contains the subsequent contact, load, and lift-off activity, and a Replace-locked Release window contains the following release and retraction. This preserves the continuous sensorimotor EEG associated with the action sequence and avoids treating each annotated phase as a separate class.

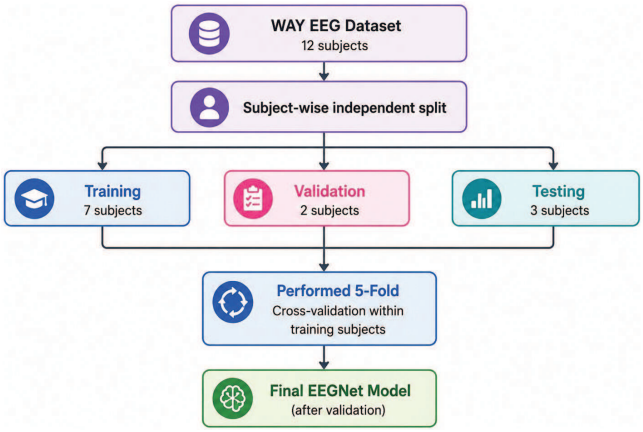
The binary mapping (Grasp vs. Release) is coarser than the original multi-event annotation, but it matches the command set required for prosthetic-style control. Consequently, the forearm rotation was programmed in the robotic prototype and not decoded as a separate EEG classification class. Thus, the activity related to rotation was included in the corresponding event-centered epoch. This choice is consistent with the continuous character of movement-related cortical activity: ERD/ERS in the $\mu$ and $\beta$ bands evolves across grasp phases rather than switching at discrete event boundaries [50].

### *3.1.3. Preprocessing pipeline*

A standardized preprocessing pipeline was applied uniformly across all subjects and runs. The preprocessing order follows the neurophysiologically motivated sequence: band-pass filtering, common average reference (CAR), and $z$-score normalization. Application of band-pass filters (4–40 Hz, order 4 Butterworth Infinite Impulse Response (IIR)) enables identification of $\mu$ (8–12 Hz) and $\beta$ (13–30 Hz) rhythms, retaining the relevant frequency range during motor-related components. This filter reduces low-frequency drifts and high-frequency noise, including muscle artifacts. CAR was performed on the chosen 8 channels in order to remove noise components common to all channels. Following that, trials were normalized using channel-wise $z$-score normalization. Segments or epochs were created from continuous EEG signals based on event markers, with each epoch being sampled at 500 Hz. Epochs were extracted based on events in the range of − 0.5 to 1.5 seconds, providing 2-second-long epochs containing 1000 samples each. The subject-level partitioning of the WAY EEG dataset into training, validation, and test sets is summarized in Figure 2.

In total, 6240 epochs from 96 EEG files belonging to 12 subjects were used in this research, including equal numbers (3120) of grasp-and-release trials. It should be highlighted that the quantity of epochs is greater than the quantity of trials conducted during the recording of the WAY EEG Grasp-and-Lift dataset. The reason behind this is that a single trial may have several events, and in the current case, epochs are extracted based on the handStart and replace events. This event-related epoch extraction procedure is quite common in EEG analyzes to capture temporally distinct neural responses. For subject-independent evaluation of

**Figure 2**
**Partitioning of the WAY EEG dataset into training, validation, and test subjects**




results, 7 subjects (3640 epochs) were randomly assigned to training sets, 2 subjects (1040 epochs) were set aside as the validation set, and 3 subjects (1560 epochs) were allocated as the test set. Such a division guarantees that no data leakage occurs. Five-fold cross-validation was applied only to the training subjects; test subjects remained completely unseen during the whole cross-validation process.

### *3.1.4. Sliding window segmentation*

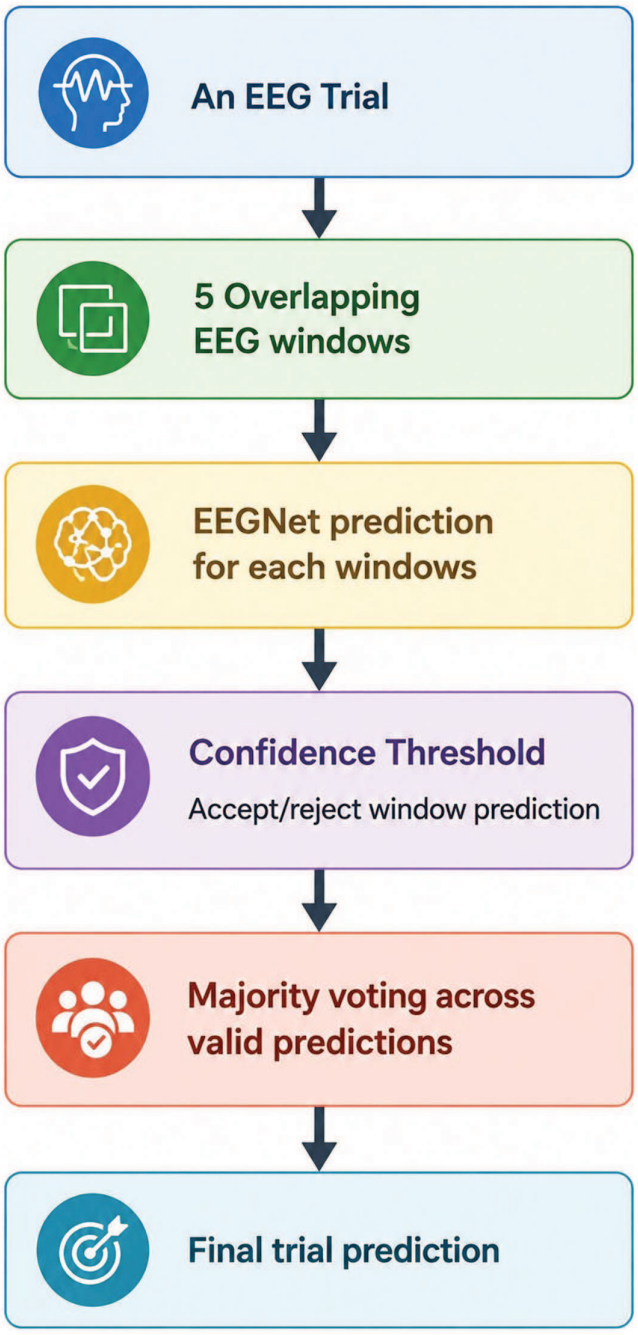
Segmentation into 5 overlapping windows with a window length of 1 second (i.e., 500 data points) was applied to each trial, thus increasing the size of the dataset and taking into account temporal features. The stride (i.e., step size) between windows is set at 125 data points (75% of the window length). Thus, using the sliding window technique, the number of training windows amounted to 18,200, validation windows amounted to 5,200, and test windows amounted to 7,800. Each window kept the original label of its trial. To prevent data leakage, sliding windows were generated independently within each subject's data after the subject-level train/validation/test split.

For trial-level evaluation, each trial of the EEG recording was divided into 5 overlapping windows and processed independently with EEGNet for obtaining the class prediction and the corresponding confidence value. If the confidence value of a certain window prediction is below the threshold, the window prediction is not included in the decision-making process. Majority voting is then applied to the list of predictions that have passed the confidence threshold to obtain the final trial-level decision between the classes of Grasp and Release. This technique helps reduce the impact of isolated erroneous predictions on the overall trial-level decision result. In case of an equal number of window predictions from both classes, the class selection rule uses the class index ordering implementation and selects the lower-indexed class in this case. The trial-level decision-making process based on confidence thresholding and majority voting is illustrated in Figure 3.

### *3.1.5. Baseline model*

For comparison purposes, the conventional baseline of Filter-Bank Common Spatial Pattern (FBCSP) features and the SVM classifier was developed. Four frequency bands were independently filtered out (4–8 Hz, 8–13 Hz, 13–30 Hz, and 30–40 Hz). Four CSP components were retained in each of the

**Figure 3**
**Trial-level decision-making using confidence thresholding and majority voting**




filter banks, and log-variance features were extracted from the CSP projections. The features from the filter banks were concatenated and normalized using the StandardScaler and classified by the Radial Basis Function (RBF)-kernel SVM with class balancing. The SVM used the fixed regularization parameter of $C = 1.0$ and gamma = 'scale'; the separate grid search and hyperparameter tuning were not performed.

For the final evaluation, the training and validation sets were used together for model fitting, whereas the three held-out test subjects were reserved for testing. Therefore, the models of FBCSP + SVM and EEGNet baselines were evaluated on the same independent test subjects. While the two methods use their specific parameterization strategies rather than identical hyperparameter tuning procedures, the test subjects were not used for model fitting. Log variance values for each CSP component were obtained, and the same preprocessing approach (band-pass filter followed by normalization) was conducted to achieve fairness while comparing with EEGNet.

## 3.2. Design and fabrication of robotic arm

The robotic hand was designed in Autodesk Fusion 360 as a five-fingered anthropomorphic structure. Six independent servo motors actuate: thumb rotation, thumb flexion, index, middle, ring, and pinky finger flexion, and forearm rotation. Each finger comprises three rigid polylactic acid (PLA) segments connected by a tendon-elastic mechanism: a fishing-line tendon routed through the palmar side drives flexion upon servo retraction, while a polyester elastic cord along the dorsal side provides passive extension return. This eliminates rigid mechanical hinges, reducing fabrication complexity and weight.

All structural components of the robotic hand were fabricated by fused deposition modeling (FDM) 3D printing using PLA, with a layer height of 0.3 mm and an infill density of 20%. Polyester elastic cord was selected as the passive extension element on the basis of its elasticity and its suitability for repeated tendon-driven finger motion, whereas fishing-line tendons were employed to transmit flexion. The assembled robotic hand was controlled by an ESP32 DevKit V1 microcontroller interfaced with a PCA9685 16-channel pulse-width-modulation (PWM) servo driver, which independently commanded six servo motors. MG90S servos were assigned to finger actuation, and MG996R servos were assigned to wrist and forearm movement. The complete prototype was realized at a materials-and-components cost of less than USD 30. This cost comparison reflects only prototype material and component expenditure and should not be interpreted as a comparison of clinical functionality, safety, sensing capability, certification, or rehabilitation performance. The resulting 3D-printed robotic hand prototype is shown in Figure 4. Following offline inference with EEGNet, the resulting binary Grasp/Release predictions were transmitted over a Universal Asynchronous Receiver-Transmitter (UART) link operating at 115200 baud to the ESP32, which then generated the corresponding servo commands through the PCA9685. The servos were programmed to travel to pre-calibrated joint positions with smooth interpolation so that grasp-and-release sequences could be executed in a continuous manner.

## 3.3. EEGNet architecture

The EEGNet model was modified to conform to the sampling frequency of 500 Hz adopted for this research. Based on the design rules of the EEGNet model, the temporal convolution kernel size is half of the sampling frequency (sfreq/2). As such, the length of the temporal convolutional kernel will be 250 samples (0.5-second receptive field), ensuring that low-frequency components of the EEG are filtered efficiently $\mu$ (8–12 Hz) and $\beta$ (13–30 Hz). The first convolutional layer carries out temporal filtering, while depthwise convolution learns spatial filters through convolution in the spatial channel. The use of separable convolution with a filter size of 50 samples (0.1 second) captures fine-temporal components. Moreover, average pooling operations are modified to (1 × 10) and (1 × 25). Other aspects of the model include batch normalization, Exponential Linear Unit (ELU) activation, and dropout (0.5) for regularization. The model receives inputs in the form of an array with a dimension of (8 × 500) representing eight EEG channels and one-second

**Figure 4**
**3D-printed robotic hand prototype**



temporal length. The training process utilizes the Adam optimization function with a learning rate of 0.001, a categorical cross-entropy loss function, a batch size of 64, and early stopping criteria of 15 epochs.

## 3.4. EEG decoding and robotic control pipeline

The suggested framework involves two temporally separated pipelines—the offline EEG classification pipeline and the online robotic command execution pathway. Such separation is necessary because EEG data were collected beforehand and used for building the model and validation. Meanwhile, further command transmission and robotic actuation were performed online.

Step 1: Offline EEG preprocessing: The previously recorded EEG signals underwent the same preprocessing procedures as those described in Section 3.1—band-pass filtering, common average referencing, and channel-wise normalization. EEG epochs were split into overlapping windows for EEGNet classification.

Step 2: Offline EEGNet inference: Preprocessed EEG windows were fed into the trained EEGNet model in order to get binary predictions (Grasp/Release). Model performance was tested using independent held-out test subjects. Therefore, due to the offline nature of EEG recording, the current classification step is an example of offline EEG inference, but not online EEG decoding.

Step 3: Online command transmission: After obtaining classification results, the generated Grasp/Release decision was translated into the corresponding command that was transmitted through the serial interface to the ESP32 controller. The communication process included command acknowledgment in order to check the transmission and execution status.

Latencies are taken into account for characterizing the temporal properties of the implemented pipeline. Software-side latency components include EEG preprocessing, EEGNet inference, and decision filtering, whereas hardware-side latency includes serial command transfer and servo actuation. The total system latency is defined as the time elapsed between the availability of an EEG processing window and the completion of the corresponding robotic actuation. The programmed servo-motion sequence requires approximately 540–600 ms, depending on the commanded motion. These values represent controller-side implementation timing specifications rather than experimentally measured physical settling times. Where direct experimental measurements of individual latency components were not available, the corresponding values are therefore reported as implementation specifications and should not be interpreted as experimentally measured latency or settling-time values.

Step 4: Online robotic actuation: Upon receiving a valid command, the ESP32 controller triggered the PCA9685 servo driver and corresponding servo motors to perform the predetermined robotic hand movement. The tendon-driven robotic hand then executed the grasp-and-release motion. Hence, hardware execution of the command represents the online component of the robotic command execution pathway following offline EEG classification. The complete offline EEG processing, command transmission, and online robotic execution pathway is summarized in Figure 5.

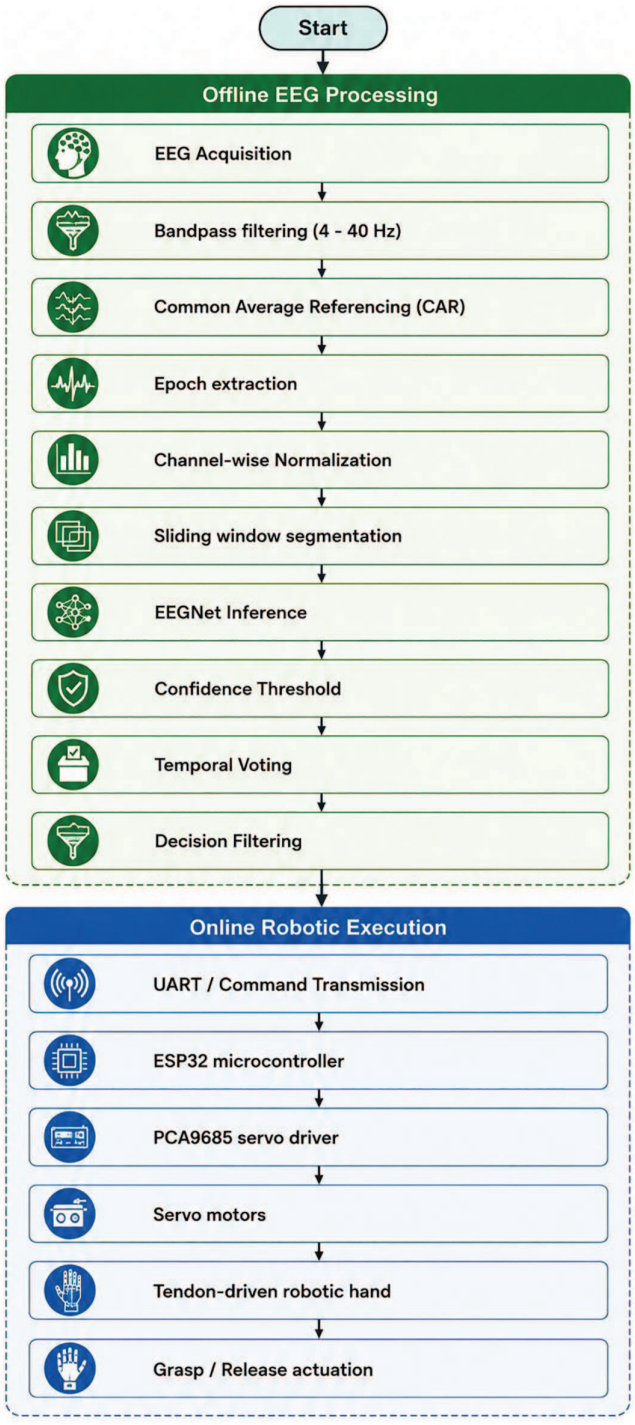
The robotic hand controller is comprised of an ESP32 DevKit V1 communicating with the desktop runtime using UART at 115,200 baud. The ESP32 communicated with the PCA9685 16-channel PWM servo driver via $I^2C$ to individually control six servo motors. MG90S miniature servos were employed for the fingers' motion, while MG996R servos were applied for the wrist and forearm motions. The tendon-driven hand incorporated PLA-printed finger segments with fishing-line tendons for flexing and polyester elastic cords for passive extension. The entire prototype was built for less than USD 30 in terms of the cost of materials and components. The tendon-driven robotic hand performing grasping and forearm rotation is shown in Figure 6.

The complete hardware configuration and specifications of the robotic arm are summarized in Table 1. Therefore, this paper does not show an example of continuous EEG acquisition and real-time EEG decoding. On the contrary, it shows how offline EEG classification can be paired with the online robotic command execution pathway as an engineering proof-of-concept.

## 4. Results

The presented EEGNet architecture obtains an accuracy of 74.74% per trial and 68.76% per time window, thus significantly exceeding the accuracy obtained using the baseline FBCSP + SVM classifier (60.38%). This finding is supported by multiple studies suggesting that an end-to-end deep learning architecture outperforms manually selected features in EEG classification due to its ability to discover the hierarchy of spatiotemporal representations. The higher information transfer rate (ITR) of 4.43

**Figure 5**
**Detailed system architecture of offline EEG processing and online robotic command transmission and execution pipeline**



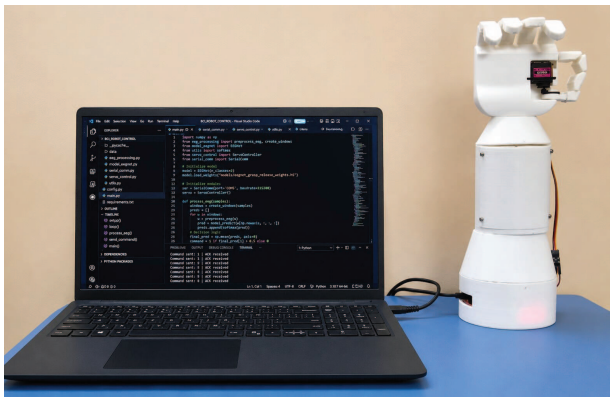

bits/min as against 0.75 bits/min for FBCSP+SVM implies higher information flow. The ITR was computed using:

$$ITR = \left(\frac{60}{T}\right) \times \left[\log_2(N) + P \log_2(P) + (1-P)\log_2\left(\frac{1-P}{N-1}\right)\right] \quad (1)$$

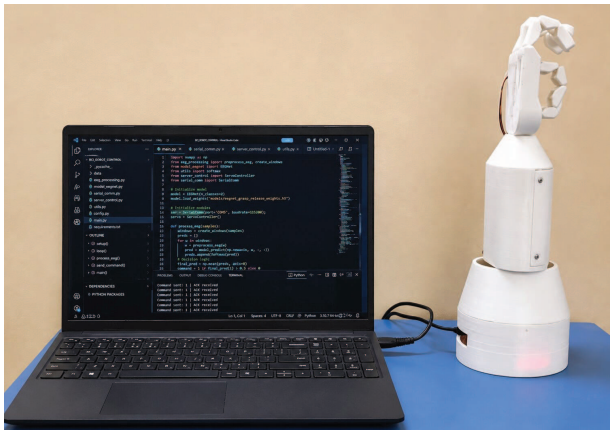
where $N$ = number of classes, $P$ = classification accuracy, and $T$ = trial duration (2.5 seconds).

**Figure 6**
**Tendon-driven robotic hand prototype and its operation: (a) grasping demonstration, and (b) forearm rotation demonstration**

(a)



(b)



The discrepancy between the accuracy from cross-validation (66.04% ± 0.62%) and the accuracy from the final held-out test (74.74%) is due to the stage at which both accuracies were evaluated. The cross-validation was used to evaluate the model accuracy within the folds of the training subjects, while the final test accuracy was evaluated using the three new test subjects.

Table 2 presents the comparison between EEGNet and the traditional FBCSP + SVM baseline method for grasp-release classification. It lists accuracy and ITR as key measures. The results clearly show that EEGNet outperforms the baseline, achieving higher accuracy and ITR. Those results show that EEGNet demonstrates better classification performance than the FBCSP + SVM baseline for the executed-movement Grasp/Release EEG task. In comparison with the FBCSP + SVM baseline, the trial-level accuracy reached by EEGNet was 74.74%, which is 60.38% for the baseline. This resulted in an absolute improvement of 14.36 percentage points.

In order to compare the predictions of EEGNet and FBCSP + SVM on the same set of 1,560 held-out test trials, a paired exact McNemar test was carried out. The test yielded a statistically significant difference between the two classifiers ($p < 0.001$). In total, 680 trials were discordant, where EEGNet classified 452 trials correctly, which had been misclassified by FBCSP + SVM, while FBCSP + SVM classified 228 trials correctly, which had been misclassified by EEGNet. Consequently, the obtained value of the paired discordance effect measure is $\Delta = 0.3294$. Table 3 depicts the FBCSP + SVM predictions on held-out trials, where the McNemar test was performed.

**Table 1**
**Hardware configuration of the robotic arm**

| Component | Specification |
|---|---|
| Microcontroller | ESP32 DevKit V1 |
| Serial communication | UART, 115,200 baud |
| Servo driver | PCA9685, 16-channel PWM |
| Driver interface | $I^2C$ |
| Number of servo motors | 6 |
| Finger servos | MG90S |
| Wrist/forearm servos | MG996R |
| Structural material | PLA, FDM 3D printing |
| Layer height | 0.3 mm |
| Infill | 20% |
| Tendon | Fishing-line tendon |
| Extension mechanism | Polyester elastic cord |
| Prototype fabrication cost | < USD 30 |

**Table 2**
**Performance comparison between EEGNet and the baseline method**

| Method | Accuracy (%) | ITR (bits/min) |
|---|---|---|
| FBCSP + SVM | 60.38 | 0.75 |
| EEGNet (window-level) | 68.76 | 4.99 |
| EEGNet (trial-level) | 74.74 | 4.43 |

**Table 3**
**Paired contingency table for EEGNet and FBCSP + SVM predictions on the held-out test set**

| | FBCSP + SVM Correct | FBCSP + SVM Wrong |
|---|---|---|
| EEGNet correct | 714 | 452 |
| EEGNet wrong | 228 | 166 |

Diagonal entries are trials where both classifiers were in accordance with the ground truth or both have produced an error in classification. Off-diagonal entries are used for the McNemar test and represent discordant predictions.

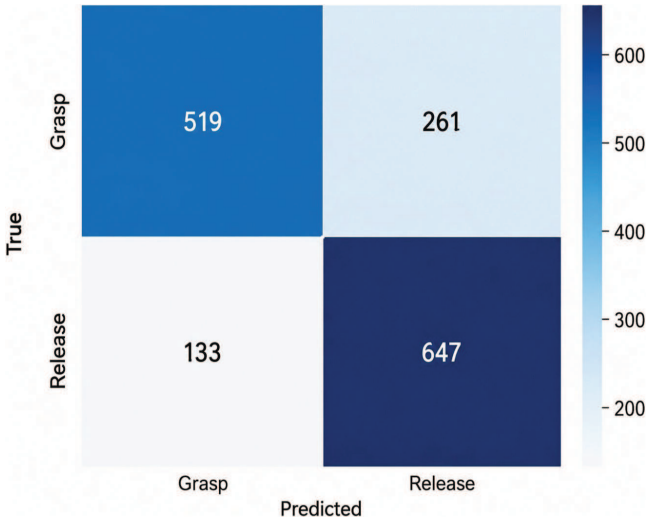
For a more thorough analysis of the binary Grasp/Release classification quality, several additional class-wise and aggregated metrics were evaluated using the holdout test set. These included precision, recall, specificity, F1-score, ROC-AUC, and balanced accuracy. Precision refers to the fraction of true predictions among all positive predictions. Recall represents the fraction of positive examples that were classified correctly. Specificity refers to the ability of the classifier to reject the opposite class. The F1-score calculates the harmonic mean of precision and recall. This metric can be particularly useful when false positives and false negatives have the same importance. Balanced accuracy refers to the arithmetic mean of sensitivity and specificity. Hence, balanced accuracy can be useful when the class distributions are unbalanced. ROC-AUC represents the discriminative ability of the classifier regardless of the decision threshold. The comprehensive class-wise and overall classification performance of EEGNet is summarized in Table 4.

**Table 4**
**Comprehensive EEGNet classification performance**

| Metric | Grasp | Release | Overall |
|---|---|---|---|
| Precision | 79.60% | 71.26% | 75.43% |
| Recall | 66.54% | 82.95% | 74.74% |
| Specificity | 82.95% | 66.54% | 74.74% |
| F1-score | 72.49% | 76.66% | 74.57% |
| Balanced accuracy | — | — | 74.74% |
| ROC-AUC | — | — | 86.40% |
| Accuracy | — | — | 74.74% |

Alongside accuracy, the performance of the classification was measured by precision, recall, specificity, F1-score, ROC-AUC, and the confusion matrix. These complementary measures allow us to assess the binary Grasp/Release classification results at the class level and at different decision thresholds. The trial-level confusion matrix for the EEGNet Grasp/Release classification is shown in Figure 7.

**Figure 7**
**Confusion matrix for EEGNet grasp/release classification**




The trial-level confusion matrix also gives more insight into the classification mistakes made. Of the 780 trials for the Grasp class, 519 trials were classified as Grasp, while 261 were falsely classified as Release. Out of 780 trials for the Release class, 647 trials were classified as Release, and 133 were falsely classified as Grasp. This shows that the recall for the Release class is higher (82.95%) as compared to Grasp (66.54%), implying that more trials of the Grasp class were falsely classified. For robotic control applications, false-Grasp predictions can cause unintended hand closing and grasping, while false-Release can cause premature release of the grasp. Both kinds of errors are important in safe assistive robotic control applications, but the former kind is particularly more important as it can cause any physical interaction with the environment through the robot. The overall trial-level EEGNet accuracy and its 95% Wilson confidence interval are presented in Table 5.

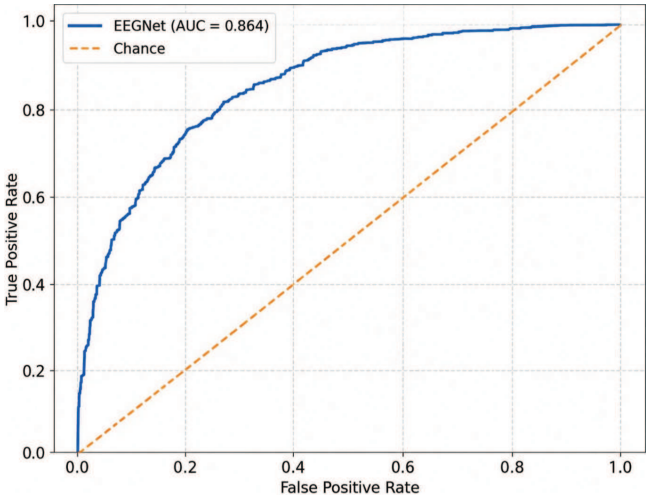
The EEGNet accuracy at the trial level was 74.74% (1166 correct classifications out of 1560 test trials), with a 95% Wilson confidence interval of 72.53–76.84%. The confidence interval

**Table 5**
**EEGNet trial-level accuracy and 95% confidence interval on the held-out test set**

| Evaluation metric | EEGNet result |
|---|---|
| Correct predictions | 1,166 |
| Total test trials | 1,560 |
| Accuracy | 74.74% |
| 95% confidence interval (Wilson) | 72.53–76.84% |

quantifies the uncertainty in pooled held-out test accuracy estimation. The ROC-AUC curve for the EEGNet Grasp/Release classification is shown in Figure 8.

**Figure 8**
**ROC-AUC curve for EEGNet grasp/release classification**




The additional metrics allow for obtaining a more elaborate assessment of the classifier performance in comparison with overall accuracy. The precision and recall values demonstrate how correctly Grasp-and-Release predictions are made considering false positive and false negative errors. The F1-score is especially important in BCI-based assistive control since it represents the combination of precision and recall and hence the balance between missing commands and false commands. Specificity additionally characterizes the ability of the classifier to reject the opposite command. Balanced accuracy represents the aggregated measure taking into account both classes. Receiver Operating Characteristic – Area Under the Curve (ROC-AUC) is a threshold-independent metric that describes the class separability. Thus, all those metrics provide a more thorough assessment of the EEGNet performance on the holdout subjects. The subject-level EEGNet performance for the three held-out test subjects is presented in Table 6.

EEGNet performance at the individual level for each subject category among the three test subjects that were withheld, showing inter-subject variability and stability of overall test accuracy.

The serial communication protocol provided a communication success rate of 98.18%, since out of 55 commands, 54 got an ACK response. No NACK responses were found, and only one command did not get any ACK, as shown in Table 7. Thus, the reported 98.18% communication success rate is a ratio of transmitted commands to commands that have got an ACK

**Table 6**
**Subject-level EEGNet performance on the held-out test subjects**

| Test subject | Number of trials | Accuracy (%) |
|---|---|---|
| Subject 1 | 520 | 79.42 |
| Subject 7 | 520 | 71.92 |
| Subject 8 | 520 | 72.88 |
| Mean ± SD | 520 per subject | 74.74 ± 4.08 |

**Table 7**
**Serial communication and hardware reliability**

| Metric | Value |
|---|---|
| Total commands | 55 |
| Successful (ACK) | 54 |
| Failed (NACK) | 0 |
| No response/timeout | 1 |
| Reliability (%) | 98.18 |

response and cannot be interpreted as physical execution accuracy.

To characterize the robotic prototype quantitatively within the limits of the available measurements, Table 8 summarizes the principal hardware specifications, programmed servo-motion timing, communication settings, and observed command-transmission results. Six servos were driven from an ESP32 through a PCA9685 interface over UART at 115 200 baud. Firmware advanced the servos in 3° steps every 10 ms, giving nominal programmed durations of about 600 ms for Rest to Grasp and 540 ms for Grasp to Release. Of 55 transmitted commands, 54 received an ACK (98.18% communication reliability). These figures describe the implemented controller and serial link. The 540–600 ms intervals are firmware timing specifications and should not be read as experimentally measured mechanical settling times.

Although the prototype executed the intended grasp, release, and forearm rotation sequences, the present study did not include a quantitative mechanical characterization. Grasp force, payload capacity, positional accuracy, cycle-to-cycle repeatability, physical servo settling time, and long-term mechanical reliability were not measured. Consequently, the reported communication reliability and the programmed 540–600 ms servo intervals must not be taken as evidence of actuation accuracy or repeatability. Those quantities require a dedicated mechanical protocol in future work, based on repeated actuation cycles, controlled payloads, and appropriate force and displacement sensors.

The measured latencies on the software side were 1.6668 ms, which includes EEG preprocessing (0.8954 ± 0.1734 ms), EEGNet inference (0.7695 ± 0.0363 ms), and decision filtering (0.0019 ± 0.0021 ms). These latencies characterize the computational part of the implemented pipeline and cannot be considered the full end-to-end system latency. UART communication latency and servo-actuation latency were not remeasured due to the unavailability of the ESP32-based hardware used previously in this study for experiments. Therefore, the total physical EEG-to-robot latency is not provided. The individual software processing latencies and the programmed servo-motion interval are summarized in Table 9.

The implemented firmware operates the servo incrementally at 3° every 10 ms. According to the programmed angular trajectories, the nominally specified controller-side movement takes

**Table 8**
**Quantitative characterization of the robotic hand prototype**

| Parameter | Value | Characterization type |
|---|---|---|
| Number of servo motors | 6 | Hardware configuration |
| Finger servo model | MG90S | Hardware specification |
| Wrist/forearm servo model | MG996R | Hardware specification |
| Microcontroller | ESP32 DevKit V1 | Hardware specification |
| Servo driver | PCA9685, 16-channel PWM | Hardware specification |
| Serial communication rate | 115,200 baud | Communication specification |
| Servo incremental motion | 3° every 10 ms | Firmware specification |
| Nominal Rest-to-Grasp movement time | ~600 ms | Programmed timing |
| Nominal Grasp-to-Release movement time | ~540 ms | Programmed timing |
| Prototype fabrication cost | < USD 30 | Material/component cost |
| Commands transmitted | 55 | Experimental |
| Commands acknowledged | 54 | Experimental |
| Communication reliability | 98.18% | Experimental |
| Physical movement accuracy | Not measured | Limitation |
| Mechanical repeatability | Not measured | Limitation |
| Grasp force/payload | Not measured | Limitation |
| Physical servo settling time | Not measured | Limitation |

approximately 600 ms from Rest to Grasp and about 540 ms from the programmed Grasp-to-Release positions. This information is based on firmware timing specifications rather than experimental measurements of the physical settling time of the servos.

## 5. Discussion

### 5.1. Interpretation of classification performance

The present hardware evaluation quantifies communication reliability and controller-side motion timing; it is not a complete mechanical performance study. The 98.18% ACK rate records successful reception of serial commands and does not establish that the hand executed those commands accurately. Likewise, the 540–600 ms servo intervals are programmed controller trajectories, not measured physical settling times. Future hardware validation should therefore report grasp force, payload capacity, positional repeatability, cycle-wise actuation success, and physical response time under representative loads.

**Table 9**
**Software latency characterization of EEG decoding**

| Stage | Latency (ms) |
|---|---|
| EEG preprocessing | $0.8954 \pm 0.1734$ |
| EEGNet inference | $0.7695 \pm 0.0363$ |
| Decision filtering | $0.0019 \pm 0.0021$ |
| Software processing subtotal | 1.6668 |
| Servo-motion sequence | ~540–600 ms |

Under subject-independent offline evaluation, EEGNet reached a trial-wise accuracy of 74.74%, 14.36 percentage points above the FBCSP + SVM baseline. The gain is consistent with end-to-end representation learning: depthwise and separable convolutions estimate spatial–temporal filters from the EEG directly, without hand-tuned, subject-specific filter banks that often fail to generalize in CSP pipelines. The corresponding ITR increased from 0.75 bits/min for FBCSP + SVM to 4.43 bits/min for trial-level EEGNet. Window-level EEGNet yielded 4.99 bits/min. Both ITR values are offline estimates derived from classification accuracy and trial duration; they are not measured online bit rates.

### 5.2. Comparative analysis with traditional deep learning approaches

The results need to be benchmarked against other MI-BCI accuracy ranges in the literature, which can vary greatly depending on the methods used and the classification task performed. Traditional ML algorithms that employ CSP followed by SVM/LDA typically have accuracy scores ranging between 60 and 80% [10, 21–23, 44]. Deep learning-based models are known to deliver improved results. Lawhern et al.'s [18] EEGNet is able to get binary accuracy rates of 77.12%, while other compact and attention-based EEG architectures have reported competitive performance [18, 26, 27].

Importantly, the proposed architecture was evaluated in a subject-independent setting within the WAY EEG Grasp-and-Lift dataset, with training and testing performed on completely different subjects without any subject-specific fine-tuning. Subject-independent evaluation of the system represents a more rigorous evaluation of cross-subject generalization and is important for translation of EEG-based assistive systems in the future [12, 37]. To compare it with the classical FBCSP + SVM model, the two models have been evaluated based on the same subject-based training and test split. The accuracy of the FBCSP + SVM model was found to be 60.38%, while that of the EEGNet model was 74.74%, implying an absolute improvement of 14.36%. Although the WAY EEG Grasp-and-Lift dataset records executed movements (stronger signals than pure MI), this proxy validation represents an initial engineering step toward future evaluation of MI-driven systems for users who are unable to execute voluntary movements.

Because the present study uses executed-movement EEG rather than motor-imagery EEG, direct numerical comparison with studies using MI paradigms should be interpreted cautiously. Differences in task paradigm, participant population, dataset,

preprocessing, and evaluation protocol can substantially influence classification performance.

The executed-movement classification experiments presented in this work must not be directly compared to motor-imagery performance since there exists a considerable difference between the two paradigms concerning the sensorimotor response elicited.

## 5.3. Methodological considerations and performance interpretation

The preprocessing steps were applied in a neurophysiologically motivated order: band-pass filtering (4–40 Hz), CAR, and then $z$-score normalization. Baseline temporal selection can also influence ERD/ERS analysis in motor-imagery BCI studies [50]. Spatial referencing was therefore confined to the motor-relevant band, which sharpens the lateralization of sensorimotor patterns. Subjects were first partitioned at the subject level into seven training, two validation, and three test participants. Cross-validation was then leakage-free: after this split, trials were windowed independently inside each fold of the training subjects only. This prevents temporal contamination between training and validation windows and avoids inflated performance estimates associated with inappropriate windowing before data splitting.

A subject-level 7/2/3 partition was used throughout. Five-fold cross-validation was applied only to the seven training subjects; the two validation subjects and the three test subjects were held out of every fold. Windowing was performed separately within each fold after this subject-level division. The resulting cross-validation accuracy was 66.04% ± 0.62%. After hyperparameter selection, the model was retrained on the combined training and validation subjects ($n = 9$) and evaluated once on the three subjects that had remained unseen. That held-out test accuracy was 74.74%. The two figures therefore reflect different stages and different subject sets; they are not interchangeable.

The inter-subject variability was evaluated by running a test of the final EEGNet model on held-out subjects (Subjects 1, 7, and 8) independently. The independent subject split was preserved throughout, and trial-level decisions were made with the same five-window majority vote as in the case of the pooled test set. Each subject produced 520 trials. Thus, the trial-level accuracies were 79.42% for Subject 1, 71.92% for Subject 7, and 72.88% for Subject 8, resulting in a mean subject-wise accuracy of 74.74% ± 4.08% (mean ± SD). It may be concluded that there is a measurable inter-subject variability. However, it does not seem that the pooled accuracy is biased toward one of the particular subjects. Since only three independent test subjects were available for the study, the results obtained should be treated as preliminary evidence of the generalization ability of the model across subjects.

## 5.4. Executed movement as a proxy for motor imagery

It is important to note that the EEG data used in this research refer to executed grasp-and-lift movements and not to motor imagery. This distinction must be made while analyzing the classification performance obtained in this work. Specifically, executed movements are known to elicit both motor cortex activity and movement-related neural responses, as well as feedback from muscles, tendons, and joints involved in the movement. These additional processes can make the executed movement classification more successful than motor imagery because it is characterized by a higher signal-to-noise ratio. Therefore, the 74.74% trial-level accuracy obtained in this work should not be taken as indicative of expected performance for motor imagery.

The use of executed movement EEG was designed merely to test an engineering proof-of-concept with regard to EEG processing, decoding, command generation, and robotic actuation. While the resulting pipeline serves as a good base for further research, the present results do not represent generalization for motor-imagery decoding, stroke subjects, and clinical rehabilitation. Future works should analyze the same pipeline on motor-imagery EEG datasets and then on datasets from people with motor impairment.

## 5.5. Limitations and clinical relevance

The present study used the EEG recordings of 12 healthy subjects, which is a rather small number of participants and might reduce the statistical power and generalizability of the achieved classification results. Specifically, the inter-subject variability of the EEG properties might not be covered with this sample. Despite the subject-independent evaluation method providing an independent evaluation with held-out subjects, it would require further validation on a larger and more diverse dataset, including patients with motor impairments, to prove its clinical applicability. Future research work will focus on investigation of the suggested solution using multi-subject and patient EEG data.

Several limitations should be acknowledged. First, the current system operates in an open-loop regime and lacks proprioceptive or haptic feedback, factors that the literature shows are important for enhancing neuroplasticity and user experience in BCI-controlled rehabilitation [20]. Second, the study used offline EEG data collected from the WAY EEG Grasp-and-Lift dataset that involved executed grasp-and-lift actions rather than motor imagery in healthy volunteers [17, 33, 36]. Third, the binary grasp/release classification, while pragmatically suited to prosthetic control, does not yet discriminate between different grasp types (e.g., power, pinch, tripod) [35, 47, 48].

However, the reliability of command transmission, cost-efficient hardware construction, and robotic movement manipulation indicate the feasibility of the proposed system as an engineering proof-of-concept. Nevertheless, the rehabilitation effectiveness remains an unexplored aspect of the current work, and future studies will have to address it through the use of EEG collection in real time, motor-impaired patients, sensory feedback, and clinical assessment. Another limitation is that the measurements of mechanical repeatability and payload capacity were not performed to be updated in the current revision. Although the prototype was successfully integrated and operated during the original hardware experiments, these characteristics are therefore not reported as newly obtained measurements of quantitative performance parameters in the present revision. In future works, servo positioning repeatability, grasp force/payload capacity, and long-term mechanical reliability will be evaluated experimentally.

The present study characterized the robotic prototype primarily as a proof-of-concept platform for command execution. Quantitative measurements of physical movement accuracy, grasp force, mechanical repeatability, long-term cycle endurance, and mechanical failure rate were not performed; consequently, the reported hardware results should not be interpreted as a comprehensive mechanical performance evaluation.

## 6. Conclusion

This study developed a proof-of-concept end-to-end EEG-BCI pipeline for grasp intention decoding using the EEGNet architecture. Trained on the WAY EEG Grasp-and-Lift dataset (executed movements), the model achieved a trial-level accuracy of 74.74% in a subject-independent setting, outperforming the FBCSP + SVM baseline. The robotic command execution pathway implementation involved online command executions after the offline EEG classification phase. The developed prototype involves a tendon-driven 3D-printed robotic hand capable of performing programmed grasp, release, and forearm rotation actions upon reception of control commands. It is essential to mention that EEG classification was conducted based on the execution-movement EEG data recorded in healthy participants. This research involved a technical feasibility demonstration of the developed EEG decoding and robotic command pipeline. The results cannot be applied directly to BCI-based motor imagery or stroke rehabilitation applications without proper experimental validation. Although the current prototype uses offline training on executed movement data and open-loop control, the demonstrated end-to-end pipeline, superior subject-independent performance, and low-cost hardware integration provide a basis for future investigation of fully wearable, closed-loop soft exoskeletons with real-time sensory feedback for stroke neurorehabilitation.

## 7. Future Works

In summary, the current research involves the creation of a tendon-driven robotic hand prototype to evaluate the efficacy of EEG decoding and robotic command pipeline integration. Classification was conducted based on execution-movement EEG data acquired from healthy subjects and not motor-imagery EEG. Future studies should focus on validating the entire pipeline on motor-imagery EEG data and conducting extensive analysis on individuals with motor impairment. Other aspects that require investigation include the online acquisition of EEG signals, real-time decoding, closed-loop control, and assessment of the robotic hand repeatability. In light of the abovementioned feasibility of the BCI pipeline, one important direction is transitioning the current rigid prototype design into a wearable soft robotic hand exoskeleton to aid in stroke patients' rehabilitation. Compared to the current rigid design, a soft robotic exoskeleton would be directly worn on the paralyzed hand, allowing for real-world actuation of the patient's limb through decoded motor intentions. By following the soft robotics approach, using pneumatically-driven or tendon structures based on flexible materials, the proposed exoskeleton will not only adapt to the anatomical features of the human hand but also prevent potential harm to the joints in case of spasticity.

BCI-driven soft exoskeleton represents a potential future approach in assistive technology. Once validated successfully, further investigations will examine the possibility of utilizing a BCI-driven soft exoskeleton in individuals with severe stroke impairment with minimal voluntary muscle activity. The future clinical trials may investigate whether a closed-loop system combining motor-imagery EEG decoding, robotic movements, and sensory feedback helps in improving motor learning and rehabilitation outcomes. In addition, the next generation of the product will include sensors for the feedback of sensations like pressure or finger bending to complete the loop for the benefit of the patients' proprioceptive senses. On the algorithmic level, more research can be done on real-time EEG input as a replacement for training based on datasets and decoding multiple classes of grasp, as well as designing an attention-based and a transfer-learning model. Finally, the effectiveness of the system in severe stroke patients needs to be confirmed by clinical trials.

## Acknowledgement

The authors thank the Department of Biomedical Engineering, Rajalakshmi Engineering College, for providing the required facilities to conduct the research.

## Ethical Statement

This study involved secondary analysis of publicly available EEG data. No new human or animal data were collected by the authors.

## Conflicts of Interest

The authors declare that they have no conflicts of interest to this work.

## Data Availability Statement

The data that support the findings of this study are openly available at https://www.kaggle.com/c/grasp-and-lift-eeg-detection/data.

## Author Contribution Statement

**Krishnakumar Sankar:** Conceptualization, Methodology, Software, Validation, Formal analysis, Investigation, Resources, Data curation, Writing – original draft, Writing – review & editing, Visualization, Supervision, Project administration. **Kanimozhi Gowtheman:** Conceptualization, Methodology, Software, Validation, Formal analysis, Investigation, Resources, Data curation, Writing – original draft. **Keerthivasan Sundararajan:** Conceptualization, Writing – original draft. **Naresh Moorthi:** Conceptualization, Writing – original draft.

## References

[1] Cheng, Y., Lin, Y., Shi, H., Cheng, M., Zhang, B., Liu, X., . . . , & Xie, W. (2024). Projections of the stroke burden at the global, regional, and national levels up to 2050 based on the Global Burden of Disease Study 2021. *Journal of the American Heart Association*, *13*(23), e036142. https://doi.org/10.1161/JAHA.124.036142

[2] Feigin, V. L., Brainin, M., Norrving, B., Martins, S., Sacco, R. L., Hacke, W., . . . , & Lindsay, P. (2022). World Stroke Organization (WSO): Global stroke fact sheet 2022. *International Journal of Stroke*, *17*(1), 18–29. https://doi.org/10.1177/17474930211065917

[3] Feigin, V. L., Roth, G. A., Naghavi, M., Parmar, P., Krishnamurthi, R., Chugh, S., . . . , & Forouzanfar, M. H. (2016). Global burden of stroke and risk factors in 188 countries, during 1990–2013: A systematic analysis for the Global Burden of Disease Study 2013. *The Lancet Neurology*, *15*(9), 913–924. https://doi.org/10.1016/S1474-4422(16)30073-4

[4] Rocha, C. D., Carneiro, I., Torres, M., Oliveira, H. P., Solteiro Pires, E. J., & Silva, M. F. (2025). Post-stroke upper limb

rehabilitation: Clinical practices, compensatory movements, assessment, and trends. *Progress in Biomedical Engineering*, *7*(4), 042001. https://doi.org/10.1088/2516-1091/adeb1e

[5] Brewer, B. R., McDowell, S. K., & Worthen-Chaudhari, L. C. (2007). Poststroke upper extremity rehabilitation: A review of robotic systems and clinical results. *Topics in Stroke Rehabilitation*, *14*(6), 22–44. https://doi.org/10.1310/tsr1406-22

[6] Wolpaw, J. R. (2004). Chapter 64 Brain-computer interfaces (BCIs) for communication and control: A mini-review. *Supplements to Clinical Neurophysiology*, *57*, 607–613. https://doi.org/10.1016/S1567-424X(09)70400-3

[7] Shih, J. J., Krusienski, D. J., & Wolpaw, J. R. (2012). Brain-computer interfaces in medicine. *Mayo Clinic Proceedings*, *87*(3), 268–279. https://doi.org/10.1016/j.mayocp.2011.12.008

[8] Chaudhary, U., Birbaumer, N., & Ramos-Murguialday, A. (2016). Brain–computer interfaces for communication and rehabilitation. *Nature Reviews Neurology*, *12*(9), 513–525. https://doi.org/10.1038/nrneurol.2016.113

[9] Cincotti, F., Mattia, D., Aloise, F., Bufalari, S., Schalk, G., Oriolo, G., . . . , & Babiloni, F. (2008). Non-invasive brain–computer interface system: Towards its application as assistive technology. *Brain Research Bulletin*, *75*(6), 796–803. https://doi.org/10.1016/j.brainresbull.2008.01.007

[10] Al-Quraishi, M. S., Elamvazuthi, I., Daud, S. A., Parasuraman, S., & Borboni, A. (2018). EEG-based control for upper and lower limb exoskeletons and prostheses: A systematic review. *Sensors*, *18*(10), 3342. https://doi.org/10.3390/s18103342

[11] Orban, M., Elsamanty, M., Guo, K., Zhang, S., & Yang, H. (2022). A review of brain activity and EEG-based brain–computer interfaces for rehabilitation application. *Bioengineering*, *9*(12), 768. https://doi.org/10.3390/bioengineering9120768

[12] Baniqued, P. D. E., Stanyer, E. C., Awais, M., Alazmani, A., Jackson, A. E., Mon-Williams, M. A., . . . , & Holt, R. J. (2021). Brain–computer interface robotics for hand rehabilitation after stroke: A systematic review. *Journal of Neuroengineering and Rehabilitation*, *18*(1), 15. https://doi.org/10.1186/s12984-021-00820-8

[13] Cervera, M. A., Soekadar, S. R., Ushiba, J., Millán, J. D. R., Liu, M., Birbaumer, N., & Garipelli, G. (2018). Brain-computer interfaces for post-stroke motor rehabilitation: A meta-analysis. *Annals of Clinical and Translational Neurology*, *5*(5), 651–663. https://doi.org/10.1002/acn3.544

[14] Zhang, M., Zhu, F., Jia, F., Wu, Y., Wang, B., Gao, L., . . . , & Tang, W. (2024). Efficacy of brain-computer interfaces on upper extremity motor function rehabilitation after stroke: A systematic review and meta-analysis. *NeuroRehabilitation*, *54*(2), 199–212. https://doi.org/10.3233/NRE-230215

[15] Qu, H., Zeng, F., Tang, Y., Shi, B., Wang, Z., Chen, X., & Wang, J. (2024). The clinical effects of brain–computer interface with robot on upper-limb function for post-stroke rehabilitation: A meta-analysis and systematic review. *Disability and Rehabilitation: Assistive Technology*, *19*(1), 30–41. https://doi.org/10.1080/17483107.2022.2060354

[16] Hu, S., Wang, F., Gao, X., Zhi, Y., & Kim, D. (2026). Effects of brain-computer interface-controlled hand robot training on post-stroke recovery of upper limb motor functions: A meta-analysis of dose-matched randomized controlled trials. *Brain Sciences*, *16*(6), 552. https://doi.org/10.3390/brainsci16060552

[17] Luciw, M. D., Jarocka, E., & Edin, B. B. (2014). Multi-channel EEG recordings during 3,936 grasp and lift trials with varying weight and friction. *Scientific Data*, *1*(1), 140047. https://doi.org/10.1038/sdata.2014.47

[18] Lawhern, V. J., Solon, A. J., Waytowich, N. R., Gordon, S. M., Hung, C. P., & Lance, B. J. (2018). EEGNet: A compact convolutional neural network for EEG-based brain–computer interfaces. *Journal of Neural Engineering*, *15*(5), 056013. https://doi.org/10.1088/1741-2552/aace8c

[19] Wang, J., Bi, L., & Fei, W. (2023). EEG-based motor BCIs for upper limb movement: Current techniques and future insights. In *IEEE Transactions on Neural Systems and Rehabilitation Engineering*, *31*, 4413–4427. https://doi.org/10.1109/TNSRE.2023.3330500

[20] Bates, M., & Sunderam, S. (2023). Hand-worn devices for assessment and rehabilitation of motor function and their potential use in BCI protocols: A review. *Frontiers in Human Neuroscience*, *17*, 1121481. https://doi.org/10.3389/fnhum.2023.1121481

[21] Alazrai, R., Alwanni, H., & Daoud, M. I. (2019). EEG-based BCI system for decoding finger movements within the same hand. *Neuroscience Letters*, *698*, 113–120. https://doi.org/10.1016/j.neulet.2018.12.045

[22] Gannouni, S., Belwafi, K., Aboalsamh, H., AlSamhan, Z., Alebdi, B., Almassad, Y., & Alobaedallah, H. (2020). EEG-based BCI system to detect fingers movements. *Brain Sciences*, *10*(12), 965. https://doi.org/10.3390/brainsci10120965

[23] Saibene, A., Caglioni, M., Corchs, S., & Gasparini, F. (2023). EEG-based BCIs on motor imagery paradigm using wearable technologies: A systematic review. *Sensors*, *23*(5), 2798. https://doi.org/10.3390/s23052798

[24] Altuwaijri, G. A., Muhammad, G., Altaheri, H., & Alsulaiman, M. (2022). A multi-branch convolutional neural network with squeeze-and-excitation attention blocks for EEG-based motor imagery signals classification. *Diagnostics*, *12*(4), 995. https://doi.org/10.3390/diagnostics12040995

[25] Hossain, K. M., Islam, M. A., Hossain, S., Nijholt, A., & Ahad, M. A. R. (2023). Status of deep learning for EEG-based brain–computer interface applications. *Frontiers in Computational Neuroscience*, *16*, 1006763. https://doi.org/10.3389/fncom.2022.1006763

[26] Autthasan, P., Chaisaen, R., Sudhawiyangkul, T., Rangpong, P., Kiatthaveephong, S., Dilokthanakul, N., . . . , & Wilaiprasitporn, T. (2022). MIN2Net: End-to-end multi-task learning for subject-independent motor imagery EEG classification. In *IEEE Transactions on Biomedical Engineering*, *69*(6), 2105–2118. https://doi.org/10.1109/TBME.2021.3137184

[27] Wu, X., Chu, Y., Li, Q., Luo, Y., Zhao, Y., & Zhao, X. (2025). AMEEGNet: Attention-based multiscale EEGNet for effective motor imagery EEG decoding. *Frontiers in Neurorobotics*, *19*, 1540033. https://doi.org/10.3389/fnbot.2025.1540033

[28] Zuo, Y., Wang, Y., Chen, D., Zomaya, A. Y., Wang, F., Gao, T., & Chen, J. (2025). High-fidelity EEG generation: Generative adversarial network highlighting time-frequency-spatial features regulated by global dynamics supervision. In *IEEE Transactions on Neural Systems and Rehabilitation Engineering*, *33*, 4432–4443. https://doi.org/10.1109/TNSRE.2025.3627436

[29] Zhang, X., Zhang, T., Jiang, Y., Zhang, W., Lu, Z., Wang, Y., & Tao, Q. (2024). A novel brain-controlled prosthetic hand method integrating AR-SSVEP augmentation, asynchronous

control, and machine vision assistance. *Heliyon*, *10*(5), e26521. https://doi.org/10.1016/j.heliyon.2024.e26521

[30] Chestek, C. A., Gilja, V., Blabe, C. H., Foster, B. L., Shenoy, K. V., Parvizi, J., & Henderson, J. M. (2013). Hand posture classification using electrocorticography signals in the gamma band over human sensorimotor brain areas. *Journal of Neural Engineering*, *10*(2), 026002. https://doi.org/10.1088/1741-2560/10/2/026002

[31] Li, M., He, B., Liang, Z., Zhao, C.-G., Chen, J., Zhuo, Y., . . . , & Althoefer, K. (2019). An attention-controlled hand exoskeleton for the rehabilitation of finger extension and flexion using a rigid-soft combined mechanism. *Frontiers in Neurorobotics*, *13*, 34. https://doi.org/10.3389/fnbot.2019.00034

[32] Likitlersuang, J., Koh, R., Gong, X., Jovanovic, L., Bolivar-Tellería, I., Myers, M., . . . , & Márquez-Chin, C. (2018). EEG-controlled functional electrical stimulation therapy with automated grasp selection: A proof-of-concept study. *Topics in Spinal Cord Injury Rehabilitation*, *24*(3), 265–274. https://doi.org/10.1310/sci2403-265

[33] Cantillo-Negrete, J., Carino-Escobar, R. I., Carrillo-Mora, P., Rodriguez-Barragan, M. A., Hernandez-Arenas, C., Quinzaños-Fresnedo, J., . . . , & Arias-Carrion, O. (2021). Brain-computer interface coupled to a robotic hand orthosis for stroke patients' neurorehabilitation: A crossover feasibility study. *Frontiers in Human Neuroscience*, *15*, 656975. https://doi.org/10.3389/fnhum.2021.656975

[34] Colucci, A., Vermehren, M., Cavallo, A., Angerhöfer, C., Peekhaus, N., Zollo, L., . . . , & Soekadar, S. R. (2022). Brain–computer interface-controlled exoskeletons in clinical neurorehabilitation: Ready or not? *Neurorehabilitation and Neural Repair*, *36*(12), 747–756. https://doi.org/10.1177/15459683221138751

[35] Ding, Y., Udompanyawit, C., Zhang, Y., & He, B. (2025). EEG-based brain-computer interface enables real-time robotic hand control at individual finger level. *Nature Communications*, *16*(1), 5401. https://doi.org/10.1038/s41467-025-61064-x

[36] Araujo, R. S., Silva, C. R., Netto, S. P., Morya, E., & Brasil, F. L. (2021). Development of a low-cost EEG-controlled hand exoskeleton 3D printed on textiles. *Frontiers in Neuroscience*, *15*, 661569. https://doi.org/10.3389/fnins.2021.661569

[37] Frolov, A. A., Mokienko, O., Lyukmanov, R., Biryukova, E., Kotov, S., Turbina, L., . . . , & Bushkova, Y. (2017). Post-stroke rehabilitation training with a motor-imagery-based brain-computer interface (BCI)-controlled hand exoskeleton: A randomized controlled multicenter trial. *Frontiers in Neuroscience*, *11*, 400. https://doi.org/10.3389/fnins.2017.00400

[38] Mattia, D., Pichiorri, F., Colamarino, E., Masciullo, M., Morone, G., Toppi, J., . . . , & Molinari, M. (2020). The Promotoer, a brain-computer interface-assisted intervention to promote upper limb functional motor recovery after stroke: A study protocol for a randomized controlled trial to test early and long-term efficacy and to identify determinants of response. *BMC Neurology*, *20*(1), 254. https://doi.org/10.1186/s12883-020-01826-w

[39] Bhagat, N. A., Venkatakrishnan, A., Abibullaev, B., Artz, E. J., Yozbatiran, N., Blank, A. A., . . . , & Contreras-Vidal, J. L. (2016). Design and optimization of an EEG-based brain machine interface (BMI) to an upper-limb exoskeleton for stroke survivors. *Frontiers in Neuroscience*, *10*, 122. https://doi.org/10.3389/fnins.2016.00122

[40] Yue, Z., Zhang, X., & Wang, J. (2017). Hand rehabilitation robotics on poststroke motor recovery. *Behavioural Neurology*, *2017*(1), 3908135. https://doi.org/10.1155/2017/3908135

[41] Cutipa-Puma, D. R., Coaguila-Quispe, C. G., & Yanyachi, P. R. (2023). A low-cost robotic hand prosthesis with apparent haptic sense controlled by electroencephalographic signals. *HardwareX*, *14*, e00439. https://doi.org/10.1016/j.ohx.2023.e00439

[42] González-España, J. J., Sánchez-Rodríguez, L., Pacheco-Ramírez, M. A., Feng, J., Nedley, K., Chang, S.-H., . . . , & Contreras-Vidal, J. L. (2025). At-home stroke neurorehabilitation: Early findings with the Neuroexo BCI system. *Sensors*, *25*(5), 1322. https://doi.org/10.3390/s25051322

[43] Fu, J., Chen, S., Shu, X., Lin, Y., Jiang, Z., Wei, D., . . . , & Jia, J. (2023). Functional-oriented, portable brain–computer interface training for hand motor recovery after stroke: A randomized controlled study. *Frontiers in Neuroscience*, *17*, 1146146. https://doi.org/10.3389/fnins.2023.1146146

[44] Fu, J., Chen, S., & Jia, J. (2023). Sensorimotor rhythm-based brain–computer interfaces for motor tasks used in hand upper extremity rehabilitation after stroke: A systematic review. *Brain Sciences*, *13*(1), 56. https://doi.org/10.3390/brainsci13010056

[45] Mokienko, O. A., Lyukmanov, R. K., Bobrov, P. D., Suponeva, N. A., & Piradov, M. A. (2023). Brain–computer interfaces for upper limb motor recovery after stroke: Current status and development prospects (Review). *Sovremennye Tehnologii v Medicine*, *15*(6), 63–73. https://doi.org/10.17691/stm2023.15.6.07

[46] Gouret, A., le, Bars., Porssut, S., Waszak, T., F, & Chokron, S. (2024). Advancements in brain-computer interfaces for the rehabilitation of unilateral spatial neglect: A concise review. *Frontiers in Neuroscience*, *18*, 1373377. https://doi.org/10.3389/fnins.2024.1373377

[47] Sankar, K., Afreen, A., & Kumar, A. S. (2026). Evaluation of natural hand movements and grasp force in prosthetic hands: A systematic review. *Smart Wearable Technology*. Advance online publication. https://doi.org/10.47852/bonviewSWT62029602

[48] Siegel, J. R., Harwood, J. K., Lau, A. C., Brenneis, D. J., Dawson, M. R., Pilarski, P. M., & Schofield, J. S. (2024). A performance evaluation of commercially available and 3D-printable prosthetic hands: A comparison using the anthropomorphic hand assessment protocol. *BMC Biomedical Engineering*, *6*(1), 11. https://doi.org/10.1186/s42490-024-00086-w

[49] Tonin, A., Semprini, M., Kiper, P., & Mantini, D. (2025). Brain-computer interfaces for stroke motor rehabilitation. *Bioengineering*, *12*(8), 820. https://doi.org/10.3390/bioengineering12080820

[50] Rimbert, S., Trocellier, D., & Lotte, F. (2023). Impact of the baseline temporal selection on the ERD/ERS analysis for motor imagery-based BCI. In *2023 45th Annual International Conference of the IEEE Engineering in Medicine & Biology Society*, 1–4. https://doi.org/10.1109/EMBC40787.2023.10340748

**How to Cite:** Sankar, K., Gowtheman, K., Sundararajan, K., & Moorthi, N. (2026). Proof-of-Concept End-to-End EEG-BCI Pipeline for Grasp-and-Release Decoding and Low-Cost Tendon-Driven Actuation. *Smart Wearable Technology*. https://doi.org/10.47852/bonviewSWT620210799